化石研究会会誌 Journal of Fossil Research, Vol. 48(2), 53-65(2016)

[Original report]

Aspects of the apatite crystal : Two pathways for apatite formation, the mechanisms underlying crystal structure defects, and the pathological calcification event

KAKEI, Mitsuo*, YOSHIKAWA, Masayoshi** and MISHIMA, Hiroyuki***

Abstract

Examination of biologically induced apatite crystals revealed three insights. 1) There are two different pathways for apatite formation : the octacalcium phosphate (OCP) pathway and the central dark line (CDL) pathway. 2) The mechanisms underlying crystal structure defects caused by exposure to harmful chemicals, such as fluoride or cadmium ions, or by estrogen deficiency, are associated with dental fluorosis and the risk of developing postmenopausal osteoporosis. 3) The recently prevalent phenotypic change theory, which proposes that soft tissue cells are converted into hard tissue forming cells under pathological conditions, was found invalid in vascular lesions. These findings are expected to contribute to resolving various controversial issues related to calcification events.

Key words : octacalcium phosphate, central dark line, crystal structure defects, osteoporosis, pathological calcification

Abbreviations : OCP : octacalcium phosphate ; CDL : central dark line ; Es : estrogen ; CA : carbonic anhydrase ; TEM : transmission electron microscope ; TGA: thermogravimetric analysis; μCT: micro-computed tomography.

1. Introduction

Biologically induced apatite crystals are divided morphologically into central dark line (CDL)-free and CDL-bearing types (Fig. 1). This morphological difference may be explained by an evolutional change in the mechanism of apatite formation (kakei *et al.*, 2007a), which is speculated to have happened during an early geological period, based on transmission electron microscope (TEM) studies of crystals obtained from fossil remains along with various hard tissues (Table 1). In addition, two different mechanisms of apatite crystal formation might have emerged

Received : August 17, 2015 : Accepted December 19, 2015

*Division of Oral Anatomy, Meikai University School of Dentistry, Saitama, Japan
**Division of Orthodontics, Meikai University School of Dentistry, Saitama, Japan
***Department of Human Life Sciences, Kochi Gakuen College, Kochi, Japan.
Corresponding author : Kakei, Mitsuo
Division of Oral Anatomy, Meikai University School of Dentistry, 1-1Keyakidai, Sakado, Saitama350-0283, Japan
Tel : 81-498-285-5511
Fax : 81-49-287-6657 (ext.424)
E-mail : m-kakei@dent.meikai.ac.jp

independently (Kakei *et al*., 2001a, 2003, 2007a).

It is widely believed that apatite crystals are formed through a series of conversions from amorphous minerals, to octacalcium phosphate (OCP), to the stable form of hydroxyapatite (Brown, 1966; Brown *et al*., 1962, 1987; Nelson *et al*., 1986, 1989; Weiss *et al*., 1981; LeGeros *et al*., 1989; Bigi *et al*., 1990; Jonsonand and Nancollas, 1992; Cuisinier *et al*., 1992; Iijima *et al*., 1992a, 1992b, 2004; Miyake *et al*., 1993; Fowler *et al*., 1993; Houllé *et al*., 1998; Barry and Kemp, 2007). Although analyses have indicated the presence of OCP in the dental calculus (GrØn *et al*., 1967; Saxton, 1968; Kani *et al*., 1983; Mishima *et al*., 1992), it has so far been difficult to morphologically demonstrate OCP in ordinary calcified hard tissues because OCP easily converts to apatite during TEM observation. Likewise, it is debatable whether CDLs are present in apatite crystals, despite several reports indicating their presence (Rönnholm, 1962; Nylen *et al*., 1963; Travis and Glimcher, 1964; Frazier, 1968; Takuma, 1969). However, recent studies have successfully settled these issues (Marshall and Lawless, 1981; Nakahara, 1982; Kakei *et al*., 2009b). The reason why CDL had not been detected in apatite crystals in studies using high magnification was clarified (Selvig, 1972, 1973; Daculsi and Kerebel, 1978): CDL was prone to damage by electron beam exposure (Nakahara and Kakei, 1983). Studies by TEM, which do not have this drawback have established that the apatite crystals in tooth enamel, dentin, and bone are the CDL-bearing type (Marshall and Lawless, 1981; Nakahara, 1982; Nakahara and Kakei, 1984, 1989b). Subsequently, our TEM study clearly showed the lattice fringes of OCP in the dental calculus and their conversion to the apatite form (Kakei *et al*., 2009b). Although the presence of OCP or OCP-like minerals at an early stage of bone mineralization has been suggested by Raman spectroscopy (Crane *et al*., 2006), it is highly unlikely that OCP can mediate the formation of CDL-bearing type crystals, because the OCP pathway for apatite formation is quite different from the CDL pathway, we describe later.

As for the process of crystal formation in various calcified hard tissues, TEM studies have clearly demonstrated that crystallization is closely associated with organic substances in processes ranging from nucleation to growth. For example, although TEM has shown numerous ribbon-shaped structures in enamel and needle-shaped minerals in dentin and bone at an early stage of crystallization, higher magnification has revealed that both the

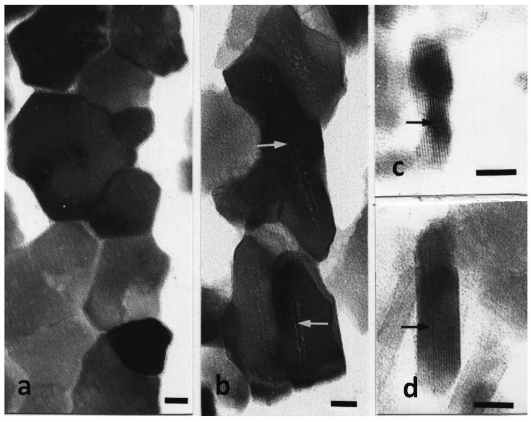

Fig. 1. Two different types of apatite crystals, CDL-free and CDL-bearing. This may reflect the different mechanisms of apatite formation. The tooth enameloid of *Scapanorhynchus texanus* consists of CDL-free apatite crystals (a), while tooth enamel (b) of *Paleoloxodon naumanni*, dentin (c), and bone (d) of *Eusthenopteron foordi* are made up of CDL-bearing apatite crystals. Arrows indicate CDLs. Bars = 10 nm, no stain.

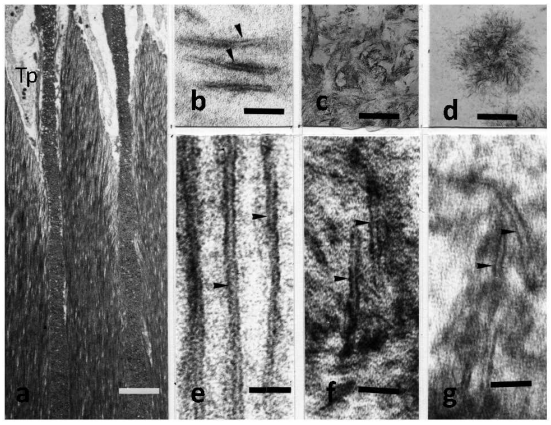

Fig. 2. TEM observations of the early stage of crystal development in rat tooth enamel, dentin, and bone. Both ribbon-shaped structures in enamel (a: cross section, b: longitudinal section) and needle-shaped minerals in dentin and bone (d and f) show the envelope structures. Arrowheads indicate the organic envelope structures. (Tp): Tomes process, (a, d and f): bar = 500 nm, (b, c, e and g): bars = 10 nm, (a-c, e and g): double stained sections, (d and f): no stain. (Modified in part from Ref. Kakei *et al.,* 2009a)

ribbon-shaped structures in enamel and the needle-shaped minerals in dentin and bone have a similar organic envelope structure as shown in figure 2 (Nakahara and Kakei 1983, 1984). In addition, TEM studies have clarified that the formation of CDL first begins as a crystal nucleation and is followed by crystal growth that occurs within an organic envelope (Figs. 3a and b). Eventually, matured crystals of tooth, dentin and bone possess CDLs in their structures (Figs. 3c-e).

This organic envelope is expected to be responsible for regulating the entire process of crystal formation. With regard to CDL formation, there has been speculation of carbonate ion involvement (Marshall and Lawless, 1981 ; Nakahara, 1982). This led us to the idea that the carbonic anhydrase (CA) enzyme, not alkaline phosphatase, might play an important role in initiating CDL formation by supplying carbonate ions (Kakei and Nakahara, 1985 ; Nakahara and Kakei, 1989 ; Kakei, 1989 ; Kakei and Nakahara, 1996 ; Kakei *et al*., 1997). Thus, the crystal nucleation process may be adversely affected if the supply of carbonate ions is insufficient or inhibited, and may cause the crystal structure defects in tooth enamel and an increase in amorphous minerals in bone. Part of our purpose in this review was to establish the nucleation process of CDL-bearing crystals. We also aimed to provide, through a presentation of the CDL pathway, a credible explanation for the mechanisms underlying crystal structure defects that result from exposure to harmful chemicals, such as F or Cd ions, or by hormonal deficiency (Kakei *et al*., 2007b, 2009a, 2013). The findings of this study have strengthened our belief that the combined effects of harmful chemicals and Es (estrogen) deficiency lead to bone fragility (Cooper *et al*., 1990; Danielson *et al*., 1992 ; Kurttio *et al*., 1999), and are related to postmenopausal osteoporosis, including Cd-induced osteoporosis or the so-called itai-itai disease (Nogawa, 1981 ; Jacobsen *et al*., 1990).

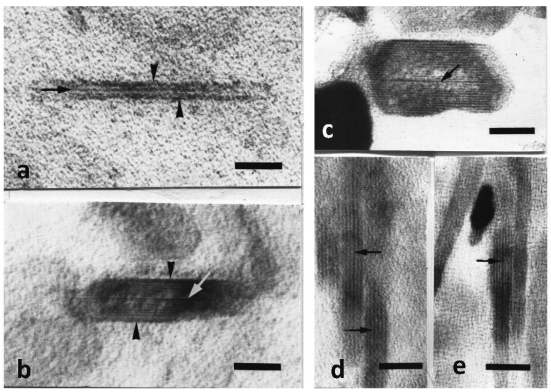

Fig. 3. TEM observations of crystal development from nucleation (a) to growth (b) in rat tooth enamel, and matured crystals of enamel (c), dentin (d) and bone (e). Crystal growth takes place within an organic envelope (arrow heads). Arrows : CDLs, arrowheads : organic envelope, bars = 10 nm, (a and b) : double stain, (c-e) : no stain.

There is a recent, growing trend to adopt the phenotypic change to explain pathological calcification (El-Labban *et al*., 1993 ; Collett *et al*., 2005 ; Kirton *et al*., 2006 ; Guerraty and Mohler, 2007 ; Danilevicius *et al*., 2007 ; Derfoul *et al*., 2006, El-Abbadi *et al*., 2007 ; Bear *et al*., 2008 ; Duer *et al*., 2008). For example, vascular calcification is also believed to occur in the same manner as bone calcification after the conversion of soft tissue cells to hard tissue-forming cells. To our knowledge, however, little is known about the detailed structure of apatite crystals generated under pathological conditions aside from one published TEM study (Faure *et al*., 1982). Many researchers advocating the phenotypic change theory have determined the calcification events by employing conventional techniques, such as von Kossa or alizarin red staining, without examining the detailed crystal structure by TEM. Such conventional staining is inadequate to confirm the crystal formation (Bonewald *et al*., 2003), eventually leading to the misconception of the calcification events. Therefore, TEM study is necessary to examine the lattice fringes of apatite crystals. If a phenotypic change occurred, a single sample of the crystal observed in a vascular lesion should be enough to confirm whether crystals are morphologically similar to bone crystals. Here, we use our findings to discuss whether a phenotypic change really takes place in pathological calcification events from the crystallographic viewpoint (Kakei *et al*., 2009c), and provide clues about some controversial issues relating to the calcification events.

2. Two pathways for apatite formation

Based on our TEM observations of the apatite crystals in various calcified hard tissues along with

Table 1. The evolution of CDL-free (-) and CDL-bearing (+) types of apatite crystals in calcified hard tissues.

Period	Species	(Class/Phylum)	Crystal type	
Pleistocene				
	Paleoloxodon naumanni	(**Mammalia**/Vertebrate)	Tooth Enamel (+)	Dentin (+)
				Bone (+)
Carboniferous				
	Mosasaurus sp.	(**Reptilia**/Vertebrate)	Tooth Enamel (+)	Dentin (+)
				Bone (+)
Devonian				
	*Xenopus laevis**	(**Amphibia**/Vertebrate)	Tooth Enamel (+)	Dentin (+)
				Bone (+)
	Eusthenopteron foordi	(**Osteichyes**/Vertebrate)	Tooth Enameloid (-)	Dentin (+)
				Bone (+)
			Dermal denticle :	
			Outer layer (-)	Inner layer(+)
Silurian				
	*Ctenacanthus occidentalis***	(**Chondrichthyes**/Vertebrate)		
			Tooth Enameloid (-)	Dentin (+)
			Placoid denticle :	
			Outer layer(-)	Inner layer(+)
Ordovician	(sample not available)			
Cambrian				
	Conodont	(**Agnatha**/Jawless vertebrate)	Tooth apparatus :	
			Enameloid (-)	Dentin(-)
	*Lingula unguis**	(**Inarticulata**/Branchiopoda)	Shell (-)	

(*) : Materials obtained from modern animals, given for a supplementary purpose. (**) : Referred to as a sample of chondrichthyes. (Modified in part from Ref. Kakei *et al.,* 2007a)

fossil materials, we concluded it was likely that two different pathways were established during an early geological period (Table 1). The CDL-free type is estimated to have arisen around the Cambrian, and later, the CDL-bearing type evolved before the Silurian and became prevalent among the vertebrates beginning with the Devonian. In the case of tooth enameloid, the transition from the CDL-free type to the CDL-bearing type seems to have taken place during the Devonian period in amphibians (Kakei *et al*., 2003). Our TEM study also gave clear evidence that the CDLs in apatite crystals have been well preserved from these geological periods due to their stability (Kakei *et al*., 2001a, 2003, 2007a).

2.1. OCP pathway

Apatite crystals are said to be formed by the conversion of OCP, a precursor mineral, despite the lack of morphological evidence so far. In this respect, our TEM study has demonstrated clearly the presence of OCP in the dental calculus (Kakei *et al*., 2009b). Also, we have confirmed morphologically the presence of OCP in both the shell of *Lingula unguis* and the radular teeth of a chiton, judging from the lattice intervals (Figs. 4b and 5a). The conversion of OCP lattice fringes into apatite lattice fringes was also confirmed by TEM observations (Figs. 4d and

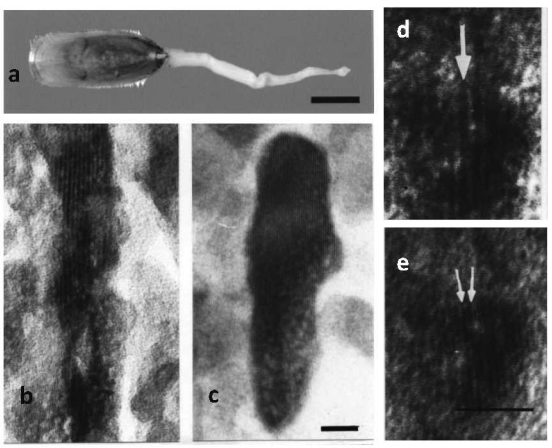

Fig. 4. OCP and apatite lattice lines and the conversion of OCP into the apatite form observed in the shell of *Lingula unguis* (a). An example of an OCP lattice line in Fig. d (arrow) that produced two apatite lattice lines in Fig. e (small arrows). (a) : bar = 1.0 cm, (b) : OCP lattice, (c) : apatite lattice, (a) : bars = 1 cm, (b = c) : bar = 10 nm, (d = e) : bar = 10 nm, (a-e) : no stain. (Modified in part from Ref. Kakei *et al.,* 2007a)

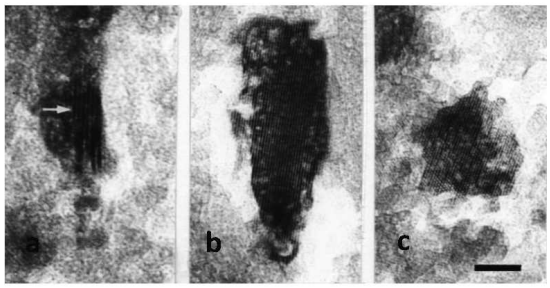

Fig. 5. TEM study on the radular teeth of a chiton. OCP lattice (a : arrow) and apatite crystals (b and c) are observed in the radular teeth of a chiton. (a = b = c) : bar = 10 nm, no stain.

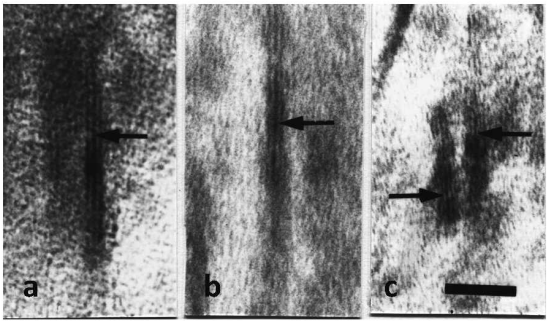

Fig. 6. TEM observations of apatite crystals in the inner layer of a shark placoid denticle (a), whale baleen (b) and goldfish scales (c), respectively. Arrows indicate CDLs. (a = b = c) : bar = 10 nm, no stain.

e), showing a stark contrast to the CDL. According to the result of the thermogravimetric analysis (TGA), the conversion of OCP to a stable apatite form easily occurs during thermal treatments at up to 150°C (Bigi *et al*., 1990). We obtained similar results by X-ray diffraction analysis demonstrating that OCP conversion occurred up to 150°C, confirming the general view that OCP is known to be thermodynamically unstable. These latest findings may serve clear evidence to differentiate between OCP and CDL. Further differences between OCP and CDL are discussed later.

CDL-free crystals created by the OCP pathway have been observed also in materials such as the conodont feeding apparatus and outer layer of a shark placoid denticle. The CDL-free crystals are considered to be capable of creating fluorapatite if F ions are present (Newesely, 1961; Brown *et al*., 1962), and these crystals are formed mainly for the exoskeleton (body protection) and for the hard part of teeth (feeding) among primitive marine creatures.

2.2. CDL pathway

Contrary to the physical properties of OCP, it has been shown by TEM analysis that CDLs in apatite crystals rapidly change their accentuated characteristics to normal apatite lattice lines and did not produce two apatite lattice lines (Nakahara and Kakei, 1983). According to our X-ray diffraction analysis coupled with TEM observation, CDLs in apatite crystals retain their features when heated to about 600°C, confirming that CDLs in apatite are more thermally stable than OCP (Kakei *et al*., 2005). Raman microprobe analysis demonstrated that the peak of 1123 cm^{-1}, which is assigned for carbonate peak of huntite minerals, $CaMg_3(CO_3)_4$, developed prior to the appearance of 960 cm^{-1} of the phosphate peak of apatite crystals at the calcification fronts of enamel, dentin and bone (Casciani *et al*., 1979). As a result, the minerals of huntite became strong candidates for the components of CDL. According to a TGA analysis of huntite minerals (Hollingbery and Hull, 2010), decomposition began at 450°C and was completed at 750°C, showing that most of the decomposition took place at about 600°C. Thus, the thermal decomposition of CDL together with the TGA profile of huntite minerals served as strong evidence that CDL is different from OCP (Kakei *et al*., 2005). We concluded that CDL consists of huntite minerals together with the initial apatite lattice line. Therefore, it is clear that CDL pathways for apatite formation developed independently following the OCP pathway during early geological periods. Moreover, the basic mechanism of CDL-bearing crystals is the same in tooth enamel, dentin and bone, as mentioned previously (Nakahara and Kakei, 1984).

The CDL-bearing crystals are also found in other types of hard tissues, such as the inner layer of a shark placoid denticle, goldfish scales and whale baleen as shown in figure 6 (Kakei *et al*., 2007a; Nakahara and Kakei 1989b). The CDL-bearing crystals seem to have spread rapidly to the endoskeleton of most vertebrates, which is necessary for bone remodeling, viewing from Table 1.

2.3. The process of crystal formation via the CDL pathway

Taking into consideration the CDL pathway,

we propose the process of crystal formation as follows (Fig. 7) : Each crystal grows within an organic envelope. This organic envelope consists of an inner mineral zone composed of calcium, phosphate and magnesium (Mg) ions, and a surrounding thin outer organic layer (Nakahara and Kakei, 1983, 1984, 1989a, Kakei *et al*., 1997). Mg ions are thought to inhibit the calcification process (LeGeros, 1981). In this respect, we speculated that Mg ions might prevent the process of nucleation from starting randomly. During the first stage of crystal development, carbonate ions supplied by CA (carbonic anhydrase) are required to initiate crystal nucleation by binding to Mg ions (Kakei *et al*., 1997, 2007b, 2009a, 2013), resulting in the formation of huntite minerals prior to the appearance of apatite lattice line at the calcification front (Casciani *et al*., 1979). Although many researchers have suspected that CA plays only a secondary role such as pH control, or plays no significant role in the process of calcification at the nucleation site (Ellison, 1965 ; Gay *et al*., 1982 ; Kumpulainen and Vaananen, 1982 ; Dogterom and Bromckers, 1982), we are convinced that CA engages directly in the crystal nucleation process as reported previously (Nakahara and Kakei, 1983, 1984, 1989a, 1989b; Kakei, 1989 ; Kakei and Nakahara, 1996 ; Kakei *et al*., 1997, 2007b, 2009a, 2013). After the formation of huntite minerals, the first apatite lattice line may be induced by reactivated calcium and phosphate ions. Next, the first lattice line together with huntite minerals may create the accentuated lattice line, the so-called central dark line (CDL), which is recognized as the nucleation site of apatite crystals. Then, an organic envelope continues to regulate the crystal growth by supplying calcium and phosphate ions. Eventually, each crystal is coated by a thin organic layer with a CDL in its structure.

Importantly, a recent Raman microprobe analysis revealed that the CDL pathway never allowed the incorporation of minor ions such as F and Cd into the crystal structure (Kakei *et al*., 2012), meaning that these minor ions randomly remained in the spaces between crystallites. The harmful effects of these ions on cellular metabolism suppressed the enzymatic activity and synthesis of some enzymes (Warburg and Christian, 1942 ; Borei, 1945 ; Cimasoni, 1972 ; Qin *et al*., 2006 ; Kakei *et al*., 2007b, 2009a, 2013). Given the detrimental effects on CA due to exposure to these ions, these findings provided an explanation to how exposure to Cd and/or F ions could be related to the development of anemia (Susheela *et al*., 2013 ; VB Rao and Vidyunmala, 2009 ; Horiguchi *et al*., 2011). Specifically, the respiratory

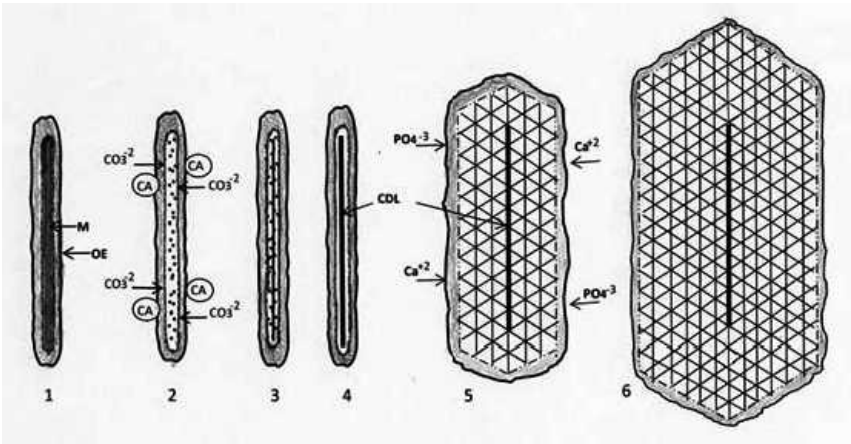

Fig. 7. Schematic representation of the apatite formation process through the CDL pathway. 1 : Amorphous mineral (M), consisting of Ca, PO4, and Mg ions within an organic envelope (OE). Mg ions : an inhibitory effect on the mineralization process. 2 : The carbonate ions supplied by carbonic anhydrase (CA) generate huntite minerals (small dots), eliminating the inhibitory effect of Mg ions. 3 : Development of first apatite lattice line. 4 : The first lattice line together with huntite minerals creates the CDL. 5 and 6 : The crystal growth following CDL formation.

role of CA in the red blood cells might be adversely affected by exposure to these chemicals. Exposure to these harmful chemicals during the crystal nucleation process results in the crystal structure defects as described in the next section.

3. The mechanisms underlying crystal structure defects

3.1. Crystal structure defects caused by harmful chemicals

We applied our CDL pathway model to evaluate the mechanism underlying crystal structure defects caused by harmful chemicals such as F and Cd ions, or due to estrogen deficiency. Immunoblot analysis revealed that both F exposure and estrogen deficiency suppressed the synthesis of CA in the enamel-forming cells, while Cd exposure decreased the enzymatic activity, provably due to the creation of Cd-binding CA (Kakei *et al*., 2009 a). Consequently, each of these factors adversely affected the crystal nucleation process. According to our differential gas pressure analysis, F exposure is considered more harmful than Cd exposure during the crystal nucleation process (Kakei *et al*., 2012).

The schematic diagram (Fig. 8A) shows the mechanism by which the declining carbonate supply causes similar crystal structural defects in developing tooth enamel, such as crystal perforation as shown in Fig. 8C (Kakei *et al*., 2007b, 2009a, 2013). These crystal structure defects can be interpreted as follows: Mg ions may retain their inhibitory effect at the central area due to an insufficient supply of carbonate ions. The peripheral area, which escapes the influence of Mg ions, can grow continuously on a base of the already formed crystal surface. Therefore, the insufficient supply of carbonate ions may be responsible for creating voids in the centers of the enamel crystals, resulting in the phenomenon of tooth bleaching, white spots on teeth, and an increase in amorphous minerals in the

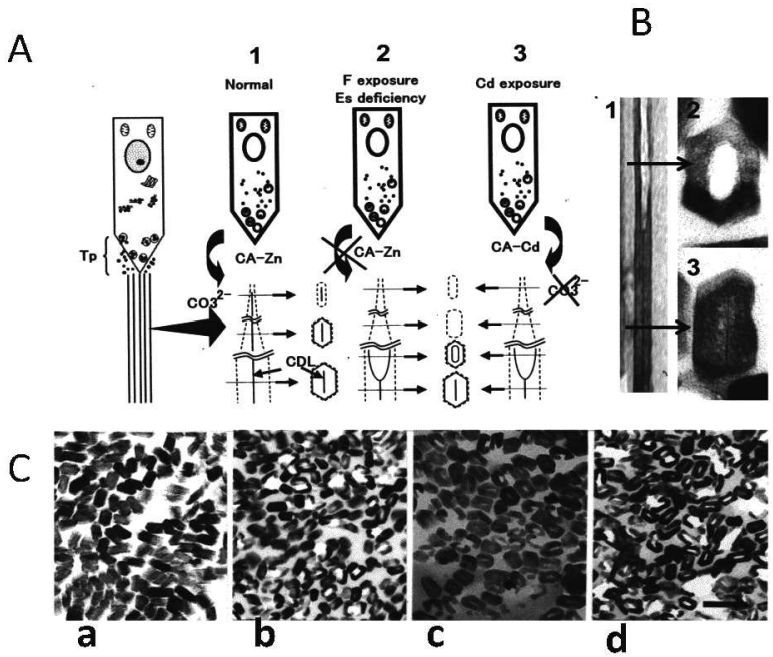

Fig. 8. Schematic of the mechanisms of crystal structure defects caused by F and Cd exposure and Es deficiency (A), and TEM observations of crystal defects in rat tooth enamel (B and C). The declining carbonate supply causes the perforated crystals in tooth enamel crystals. (Tp) : Tomes process, (CDL) : Central dark line, (A-1) : control, (A-2) : F exposure or Es deficiency, (A-3) : Cd exposure. (B-1) : Low magnification of a longitudinal section of crystal defect, (B-2 and -3) : Higher magnification of cross sections equivalent to each arrow. (C-a) : sound crystal, (C-b) : F exposure, (C-c) : Es deficiency, (C-d) : Cd exposure, (a-d) : bar = 0.5 cm.

bone (Kakei *et al*., 2007b, 2009a, 2012, 2013). Regarding the crystals purported to be the acid resistant causing by F exposure, this phenomenon is merely superficial, due to the formation of a number of perforated crystals associated with dental fluorosis. This is because the central area in the crystal is relatively less acid resistant than the peripheral area, making it a caries susceptible site (Arends and Jongebloed, 1977 ; Voegel and Frank, 1977 ; Palamara *et al*., 1986). Therefore, the phenomenon that F intake contributes to the creation of acid resistant crystals is obviously a misconception. Exposure to Cd ions is also reported to be cause the tooth bleaching due to a crystal structure defect, according to the animal studies (Wilson and Deeds, 1939 ; Kakei *et al*., 2009a). In addition, these harmful chemicals are responsible for accelerating bone fragility in postmenopausal women, as described in the next section.

3.2. Combination effects of estrogen deficiency and harmful chemicals on the bone

Es (estrogen) deficiency is generally considered a major contributing factor for the development of osteoporosis in postmenopausal women, and a factor that adversely affects osteoblastic differentiation (Robinson *et al*., 1997). Soft X-ray studies showed that the combined effects of Es deficiency and F or Cd exposure increased radiolucent areas compared to those in the control or with Es deficiency alone, creating a labyrinthine pattern in the rat calvaria (Figs. 9c and d). In addition, TEM study revealed that although the radiolucent areas in the calvaria were filled with needle-shaped minerals at low magnification (Fig. 10c), they remained in an amorphous state (Fig. 10f), while the radiopaque areas consisted of solid crystals at high magnification (Fig. 10e). The same results were observed in a sample of Es deficiency + F 1.0 ppm exposure (data not shown). This indicates that exposure to these chemical substances contributed greatly to the increase in amorphous minerals. In addition, it was noted that the radiolucent areas were not created by bone absorption with osteoclasts, suggesting the deterioration of crystal formations. Using micro-computed tomography (μCT), it has been revealed that Es deficiency resulted in declining trabecular architecture in the tibia, clearly showing osteoporotic

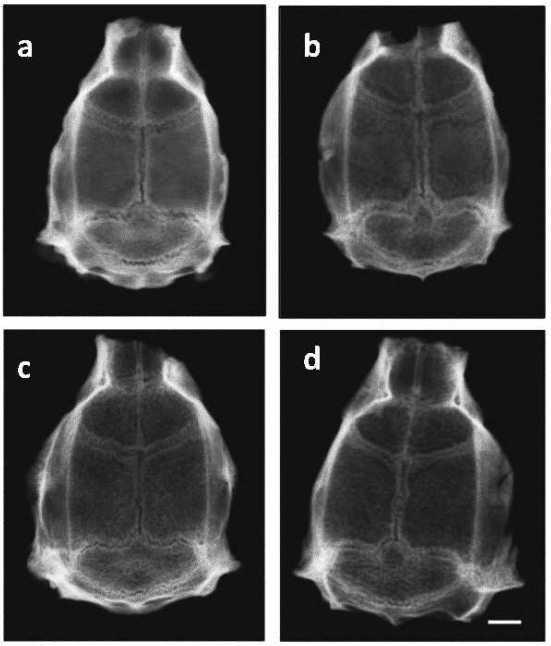

Fig. 9. Soft X-ray analysis of the combined effects of Es deficiency and F (1.0 ppm) or Cd (100 ppm) exposure on the rat calvaria. The combined effects of Es deficiency and F-1.0 ppm or Cd-100 ppm exposure increase the radiolucent areas compared to other cases (c and d). (a) : control, (b) : Es deficiency, (c) : Es deficiency+ F-1.0 ppm, (d) : Es deficiency + Cd-100 ppm, (a-f) : bar = 1 cm. (Modified from Ref. Kakei *et al.,* 2009a)

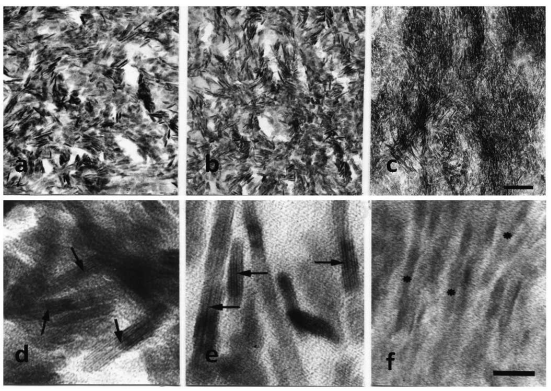

Fig. 10. TEM studies on the crystals of rat calvaria obtained from the control and the combined effects of Es deficiency and Cd (100 ppm) exposure. The radiopaque areas in the experimental and control rats consist of sound crystals showing CDLs while the radiolucent areas are filled with amorphous minerals. (a) : the control, (b and c) : Es deficiency + Cd-100 ppm, (d) : crystals of the control group, (e) : crystals of the Es deficiency + Cd-100 ppm group, (f) : amorphous minerals in the radiolucent areas of the same experimental group. Arrows indicate CDLs, (Figs. d and e). Asterisks in Fig. f show amorphous minerals. (a- c) : bar = 100 nm, (d- f) : bar = 10 nm, no stain. (Modified from Ref. Kakei *et al.,* 2013)

change. The deterioration of trabecular architecture progressed when Es deficiency was combined with exposure to F or Cd ions (Kakei *et al*., 2013). From these findings conducted under our experimental conditions, we conclude that the decline in bone formation was due to the failure of mineralization, rather than the excessive bone resorption by osteoclasts, which is generally believed to be the main cause, and might be a primary factor leading to bone fragility seen in such conditions as osteomalacia and osteoporosis.

4. The pathological calcification event

Concerning the pathological calcification of soft tissues, the so-called phenotypic change theory that soft tissue cells convert into hard tissue-forming cells has gained momentum recently. Many researchers have put too much focus on the mechanism of pathological mineralization based on this theory. Despite a large volume of research in the area, there is little specific information on the detailed crystal structure of pathological mineralization. A report describing the apatite crystals in vascular lesions had only mentioned the presence of apatite crystals, without evaluating whether they were CDL-free or CDL-bearing types (Faure *et al*., 1982). This is because the phenotypic change theory had not been introduced at that time. To verify this theory, therefore, we examined the detailed structure of apatite crystals in vascular lesion. Our findings revealed that the debris originated from the degeneration of cells that were observed in the calcified deposit (Fig. 11a). Regarding the pathologically induced apatite crystals, both types of crystal characteristic crystal types, CDL-free and CDL-bearing, were confirmed (Figs. 11b-f). Furthermore, the crystals were of various sizes, some showed lattice defects (Fig. 11e), and unknown mineral deposits were observed (data not shown), providing clear evidence that ectopic calcification definitely occurred in a manner other than the osteogenesis of ordinary calcified hard tissues. The process of pathological calcification, therefore, seems to be accompanied primarily by the degeneration of cells. In this regard, the vascular calcification seemed to occur in a similar manner as accumulation of dental calculus following bacterial death. This also generated both two types of apatite crystals (Kakei

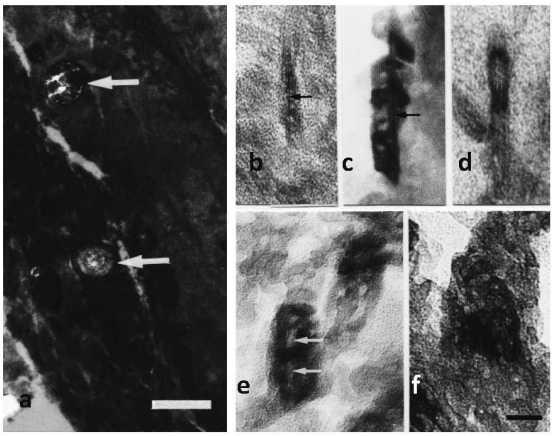

Fig. 11. TEM observations of the crystals generated during the vascular calcification. The calcified deposits contain cellular debris (white large arrows in Fig. a), and both CDL-bearing and CDL-free crystals are observed in the vascular lesion (b-f). Small arrows in Figs. b and c indicate CDLs. Crystal (b and c): CDL-bearing crystals, (d-f) : CDL-free crystals. White small arrows in Fig. e show apatite crystal with void space. (a) : bar = 0.5 μm, (b～f) : bar = 10 nm, no stain. (Modified in part from Ref. Kakei *et al.,* 2009c)

et al., 2001b, 2009c). Taking these findings into consideration, we speculate that the cellular components have the potential to generate both types of crystals after degeneration, and thus, cellular phenotypic changes appear to seldom occur during the pathological calcification events.

5. Conclusions

Among the calcified hard tissues in which apatite crystals are formed, two different pathways for apatite formation, the OCP- and the CDL-pathway, might have been established independently during an early geological time. The biologically induced apatite crystals are formed in association with the organic envelope structure, regardless of the specific pathway. In the CDL pathway, the CA enzyme initiates the nucleation process by supplying the carbonate ions. The CDL pathway for calcification may be suitable for assessing the causal relationship between bone disease, such as osteoporosis, and exposure to chemical substances and hormonal deficiencies. The apatite crystals observed in the vascular lesion were composed of both CDL-free and CDL-bearing crystals, and it is not plausible to suggest that a phenotypic change occurred. Finally, although conventional techniques such as von Kossa

and alizarin red staining are the most widely employed methods to assess calcification events, they make it difficult to clarify whether the crystals have really formed or not. Therefore, we strongly emphasize that TEM study of the detailed crystal structure will be required to evaluate various calcification events.

Acknowledgements

The primary author would like to expresses his greatest thanks to the late Prof. Hiroshi Nakahara, for his excellent guidance for working in the field of calcified hard tissues. This study was supported in part by Grant for Supporting Project for Strategic Research from the Japanese Ministry of Education, Culture, Sports, Science and Technology (2008-2012), S0801032. We greatly appreciate the valuable assistance provided by the members of Laboratory for Electron Beam Research and Application (LEBRA) at Nihon University.

References

Arends, J. and Jongebloed, W.L. (1977) Mechanism of enamel dissolution and its prevention. *J. Biol. Buccale* **5**, 219-237.

Barry, J.C. and Kemp, A. (2007) High resolution transmission electron microscopy of developing enamel in the Australian lungfish, Neoceratodus forsteri (Osteichthyes : Diponi). *Tissue Cell* **39**, 387-398.

Bear, M., Butcher, M. and Shaughnessy, S.G. (2008) Oxidized low-density lipoprotein acts synergistically with beta-glycerophosphate to induce osteoblast differentiation in primary cultures of vascular smooth muscle cells. *J. Cell Biochem.* **105**, 185-193.

Bigi, A., Cojazzi, G., Gazzano, M., Ripamonti, A. and Roveri, N. (1990) Thermal conversion of octacalcium phosphate into hydroxyapatite. *J. Inorganic Biochemistry* **40**, 293-299.

Bonewald, L.F., Harris, S.E., Rosser, J., Dallas, S.L., Camacho, N.P., Boyan, B. and Boskey, A. (2003) von Kossa staining alone is not sufficient to confirm that mineralization in vitro represents bone formation. *Calcif. Tissue Int.* **72**, 537-547.

Borei, H. (1945) Inhibition of cellular oxidation by fluoride. *Ark. Kemi. Minerl. Geol.* **20A**, 1-215.

Brown, W.E. (1966) Crystal growth of bone mineral. *Clin. Orthop.* **44**, 205-220.

Brown, W.E., Eidelman, N. and Tomazic, B. (1987) Octacalcium phosphate as a precursor in biomineral formation. *Adv. Dent. Res.* **1**, 306-313.

Brown, W.E., Smith, J.P., Lehr, J.R. and Frazier, L.A. W. (1962) Octacalcium phosphate and hydroxyapatite, *Nature* **196**, 1048-1055.

Casciani, F.S., Etz, E.S., Newbury, D.E. and Doty, S.B. (1979) Raman microprobe studies of two mineralizing tissues: Enamel of the rat incisor and the embryonic chick tibia. *Scan Electron Microsc.* **2**, 383-391.

Cimasoni, G. (1972) The inhibition of enolase by fluoride in vitro. *Caries Res.* **6**, 93-102.

Collett, G.D. and Canfield, A.E. (2005) Angiogenesis and pericytes in the initiation of ectopic calcification. *Circ. Res.* **96**, 930-938.

Cooper, C., Wickham, C., Lacey, R.F. and Barker, D.J.P. (1990) Water fluoride concentration and fracture of the proximal femur. *J. Epidemiol. and Community Health* **44**, 17-19.

Crane, N.J., Popescu, V., Morris, M.D., Steenhuis, P. and Ignelzi, M.A.jr. (2006) Raman spectroscopic evidence for octacalcium phosphate and other transient mineral species deposited during intramembranous mineralization. *Bone* **39** (3), 434-442.

Cuisinier, F.J.G., Steuer, P., Senger, B., Voegel, J.C. and Frank, R.M. (1992) Human amelogenesis. 1 : High resolution electron microscopy study of ribbon-like crystals. *Calcif. Tissue Int.* **51**, 259-268.

Daculsi, G. and Kerebel, B. (1978) High-resolution electron microscope study of human enamel crystallites : size, shape, and growth. *J. Ultrastruct. Res.* **65**, 163-172.

Danielson, C., Lyon, J.L., Egger, M. and Goodenough, G.K. (1992) Hip fractures and fluoridation in Utah's elderly population. *JAMA* **268**, 746-748.

Danilevicius, C.F., Lopes, J.B. and Pereira, R.M. (2007) Bone metabolism and vascular calcification. *Braz. J. Med. Res.* **40**, 435-442.

Derfoul, A., Perkins, G.L., Hall, D.J. and Tuan, R.S. (2006) Glucocorticoids promote chondrogenic differentiation of adult human mesenchymal stem cells by enhancing expression of cartilage extracellular matrix genes. *Stem Cells*. **24**, 1487-1495.

Dogterom, A.A. and Bromckers, A.L. (1983) Carbonic anhydrase in developing hamster molars. *J. Dent. Res.* **62**, 789-791.

Duer, M.J., Friscic, T., Proudfoot, D., Reid, D.G., Schoppet, M., Shanahan, C.M. Skepper, J.N. and Wise, E.R. (2008) Mineral surface in calcified plaque is like that of bone : further evidence for regulated mineralization. *Arteriosler. Thromb. Vasc. Biol.* **28**, 2030-2034.

El-Abbadi, M. and Giachelli, C.M. (2007) Mechanisms of vascular calcification. *Adv. Chronic Kidney Dis.* **14**, 54-66.

El-Labban, N.G., Hopper, C. and Barber, P. (1993) Ultrastructural finding of vascular degeneration in myositis ossificans circumscripta (fibrodysplasia ossificans). *J. Oral Pathol. Med.* **22**, 428-431.

Ellison, A.G. (1965) Determination of carbonic anhydrase in the epiphysis of endochondral bone. *Proc. Soc. Exp. Biol. Med.* **120**, 415-418.

Faure, G., Daculsi, G., Netter, P., Gaucher, A. and Kerebel, B. (1982) Apatites in heterotopic calcification. *Scanning Electron Microscopy* **4**, 1629-1634.

Fowler, B.O., Marković, M. and Brown, W.E. (1993) Octacalcium phosphate. 3. Infrared and Raman vibrational spectra. *Chem. Mater.* **5**, 1417-1423.

Frazier, P.D. (1968) Adult human enamel: An electron microscopic study of crystallite size and morphology. *J. Ultrastruct. Res.* **22**, 1-11.

Gay, C.V., Anderson, R.E., Schraer, H. and Howell, D. S. (1982) Identification of carbonic anhydrase in chick growth-plate cartilage. *J. Histochem. Cytochem.* **30**, 391-394.

GrØn, P., van Campen, G.J. and Lindstrom, I. (1967) Human dental calculus: inorganic chemical and crystallographic composition. *Archs. Oral Biol.* **12**, 829-837.

Guerraty, M. and Mohler, E.R.III. (2007) Models of aortic valve calcification. *J. Investig Med.* **55**, 278-283.

Hollingbery, L.A. and Hull, T.R. (2010) The thermal decomposition of huntite and hydromagnesite- a review. *Thermochimica Acta* **509**, 1-11.

Horiguchi, H., Oguma, E. and Kayama, F. (2011) Cadmium induces anemia through interdependent progress of hemolysis, body iron accumulation, and insufficient erythropoietin production in rats. *Toxicological Sciences* **122**, 198-210.

Houllé, P., Steuer, P., Voegel, J.C. and Cuisinier, F.J.G. (1998) First experimental evidence for human dentine crystal formation involving conversion of octacalcium phosphate to hydroxyapatite. *Acta Cryst.* **D54**, 1377-1381.

Iijima, M. and Moradian-Oldak, J. (2004) Control of octacalcium phosphate and apatite crystal growth by amelogenin matrices. *J. Mater. Chem.* **14**, 2189-2199.

Iijima, M., Tohda, H. and Moriwaki, Y. (1992a) Growth and structure of lamellar mixed crystals of octacalcium phosphate and apatite in a model system of enamel formation. *J. Crystal Growth* **116**, 319-326.

Iijima, M., Tohda, H., Suzuki, H., Yanagisawa, T. and Moriwaki, Y. (1992b) Effects of Fon apatite-octacalcium phosphate intergrowth and crystal morphology in a model system of tooth enamel formation. *Calcif. Tissue Int.* **50**, 357-361.

Jacobsen, S., Goldberg, J., Miles, T.P., Brody, J.A., Stiers, W. and Rimm, A.A. (1990) Regional variation in the incidence of hip fracture. US white women aged 65 years and older. *JAMA* **264**, 500-502.

Jonsonand, M.S. and Nancollas, G.H. (1992) The role of brushite and octacalcium phosphate in apatite formation. Crit. Rev. *Oral Biol. Med.* **3**, 61-82.

Kakei, M. (1989) The role of carbonic anhydrase in mineralization process of rat hard tissues. Doctor Thesis, Univ. Tokyo Metropolitan.

Kakei, M. and Nakarhara, H. (1985) Electroimmunoblotting study of carbonic anhydrase in developing enamel and dentin of the rat incisor. *Jpn. J. Oral Biol.* **27**, 357-361.

Kakei, M. and Nakaraha, H. (1996) Aspects of carbonic anhydrase and carbonate content during mineralization of the rat enamel. *Biochim. Biophys. Acta* **1289**, 226-230.

Kakei, M., Nakahara, H., Kumegawa, M., Mishima, H. and Kozawa, Y. (2001a) High-resolution electron microscopy of the crystallites of fossil enamels obtained from various geological ages. *J, Dent, Res.* **80**, 1560-1564.

Kakei, M., Nakahara, H., Kumegawa, M., Mishima, H. and Kozawa, Y. (2003) Ultrastructural study on the lattice images of calcium phosphate minerals in fossil tooth, In : Kobayashi, I. and Ozawa, H. (eds) *Proceedings of the 8th international symposium on biomineralization : formation, diversity, evolution and application,* pp. 364-368, Tokai Univ. Press, Kanagawa.

Kakei, M., Nakahara, H., Kumegawa, M., Yoshikawa, M. and Kunii, S. (2001b) Demonstration of the

central dark line in crystals of dental calculus. *Biochim. Biophys. Acta* **1524**, 189-195.

Kakei, M., Nakahara, H., Tamura, N., Itoh, H. and Kumegawa, M. (1997) Behavior of carbonate and magnesium ions in the initial crystallites at the early developmental stages of the rat calvaria. *Ann. Anat.* **179**, 311-316.

Kakei, M., Sakae, T., and Mishima, H. (2007a) Changes in biological apatite formation during the evolution of hard tissues, In: Arias, J.L. and Fernandez, M.S. (eds), *Biomineralization: from paleontology to materials Science*, pp. 107-115, Editorial Universitaria, Santiago.

Kakei, M., Sakae, T., Mishima, H. Yoshikawa, M. (2009c) Ultrastructure of apatite crystals formed during vascular calcification in humans. *J, Hard Tissue Biology* **18**, 135-140.

Kakei, M., Sakae, T. and Yoshikawa, M. (2009a) Mechanism of cadmium induced crystal defects in developing rat tooth enamel. *Proc. Jpn. Acad,* Ser. B **85**, 500-507.

Kakei, M., Sakae, T. and Yoshikawa, M. (2009b) Electron microscopy of octacalcium phosphate in the dental calculus. *J. Electron Microscopy* **58**, 393-398.

Kakei, M., Sakae, T. and Yoshikawa, M. (2012) Aspects regarding fluoride treatment for reinforcement and remineralization of apatite crystals. *J, Hard Tissue Biology* **21**, 257-265.

Kakei, M., Sakae, T. and Yoshikawa, M. (2013) Combined effects of estrogen deficiency and cadmium exposure on calcified hard tissues: animal model relating to itai-itai disease in postmenopausal women. *Proc. Jpn. Acad,* Ser. B **89**, 340-347.

Kakei, M., Sakae, T., Yoshikawa, M. and Tamura, N. (2005) Physical properties of the central dark lines in biological apatite of vertebrate calcified tissues and synthetic octacalcium phosphate. *J. Fossil Res.* **38**, 43-48.

Kakei, M., Sakae, T., Yoshikawa, M. and Tamura, N. (2007b) Effect of fluoride ions on apatite crystal formation in rat hard tissues. *Ann. Anat.* **189**, 175-81.

Kani, T., Kani, M., Moriwaki, Y. and Doi, Y. (1983) Microbeam x-ray diffraction analysis of dental calculus. *J. Dent. Res.* **62**, 92-95.

Kirton, J.P., Wilkinson, F.L., Canfield, A.E. and Alexander, M.Y. (2006) Dexamethasone down regulates calcification-inhibitor molecules and accelerates osteogenic differentiation of vascular pericytes: implications for vascular calcification. *Circ. Res.* **98**, 1264-1272.

Kumpulainen, T. and Vaananen, H.K. (1982) Immunohistochemical demonstration of extracellular carbonic anhydrase in epiphyseal growth cartilage. *Calcif. Tiss. Int.* **34**, 428-430.

Kurttio, P., Gustavsson, N., Vartiainen, T. and Pekkanen, J. (1999) Exposure to natural fluoride in well water and hip fracture : a cohort analysis in Finland. *Am. J. Epidemiol.* **150**, 817-824.

LeGeros, R.Z. (1981) Apatites in biological systems. *Prog. Crystal Growth Charact.* **4**, 1-45.

LeGeros, R.Z., Daculsi, G., Orly, I., Abergas, T. and Torres, W. (1989) Solution-mediated transformation of octacalcium phosphate (OCP) to apatite. *Scanning Microscopy* **3**, 129-138.

Marshall, A.F. and Lawless, K.R. (1981) TEM study of the central dark line in enamel crystallites. *J. Dent. Res.* **60**, 1773-1782.

Mishima, H., Yamamoto, H. and Sakae, T. (1992) SEM, energy dispersive spectroscopy and XRD analysis of human salivary calculus. *Scanning Microsc,* **6**, 487-493.

Miyake, Y., Shimoda, S. Fukae, M. and Aoba, T. (1993) Epitaxial overgrowth of apatite crystals on the thin-ribbon precursor at early stages of porcine enamel mineralization. *Calcif. Tissue Int.* **53**, 249-256.

Nakahara, H. (1982) Electron microscopic studies of the lattice image and central dark line of crystallites in sound and carious human dentin. *Josai Shika Daigaku Kiyo* **11**, 209-15.

Nakahara, H. and Kakei, M. (1983) The central dark line in developing enamel crystallite : An electron microscopic study. *Josai Shika Daigaku kiyo* **12**, 1-7.

Nakahara, H. and Kakei, M. (1984) TEM observations on the crystallites of dentin and bone. *Josai Shika Daigaku Kiyo* **13**, 259-263.

Nakahara, H. and Kakei, M. (1989a) Central dark line and carbonic anhydrase: Problems relating to crystal nucleation in enamel. In : Fearnhead, R.W. and Suga, S. (eds), *Tooth Enamel* 4, pp. 42-46, Elsevier, Amsterdam.

Nakahara, H. and Kakei, M. (1989b) Ultrastructural and protein aspects of apatite formation in vertebrate

hard tissues. In: Crick, R.E. (ed), *Origin, Evolution and Modern Aspects of Biomineralization in Plants and Animals,* pp. 225-235, Plenum Press, New York.

Nelson, D.G.A., Barry, J.C., Shields, C.P., Glena, R. and Featherstone, J.D.B. (1989) Crystal morphology, composition, and dissolution behavior of carbonated apatites prepared at controlled pH and temperature. *J. Colloid and interface Science* **130**, 467-479.

Nelson, D.G.A., Wood, G.J. and Barry, J.C. (1986) The structure of (100) defects in carbonated apatite crystallites: A high resolution electron microscope study. *Ultramicroscopy* **19**, 253-266.

Newesely, H. (1961) Darstellung von"Oktacaleciummphosphat" (tetracalcium-hydrogentriphosphat) duch homogene Krisyallisation. *Monatsh Chem.* **89**, 1020-1023.

Nogawa, K. (1981) Itai-itai disease and follow-up studies, In: J.O. Nriagu (ed), *Cadmium in the environment. Part II: Health effects,* pp. 1-37, Wiley, New York.

Nylen, U.M., Evans, E.D. and Omnell, K.A. (1963) Crystal growth in rat enamel. *J. Cell Biol.* **18**, 109-123.

Palamara, J., Phakey, P.P., Rachinger, W.A. and Orams, H.J. (1986) Ultrastructure of the intact surface zone of white spot and brown spot carious lesions in human enamel. *J. Oral Pathol.* **15**, 28-35.

Qin, J., Chai, G., Brewer, J.M., Lovelace, L.L. and Lebioda, L. (2006) Fluoride inhibition of enolase: crystal structure and thermodynamics. *Biochemistry* **45**, 793-800.

Robinson, J.A. Harris, S.A. Riggs B.L., and Spelsberg, T.C. (1997) Estrogen regulation of human osteoblastic cell proliferation and differentiation. *Endocrinology* **138**, 2919-2927.

Rönnholm, E. (1962) The amelogenesis of human teeth as revealed by electron microscopy. II The development of the enamel crystallites. *J. Ultrastruct. Res.* **6**, 249-303.

Saxton, C.A. (1968) Identification of octacalcium phosphate in human dental calculus by electron diffraction. *Archs. Oral. Biol.* **13**, 243-246.

Selvig, K.A. (1972) The crystal structure of hydroxyapatite in dental enamel as seen with the electron microscope. *J. Ultrastruct. Res.* **41**, 369-375.

Selvig, K.A. (1973) Electron microscopy of dental enamel: analysis of crystal lattice images. *Z. Zellforsch.* **137**, 271-280.

Susheela, A.K., Mondal, N.K. and Singh, A. (2013) Exposure to fluoride in smelter workers in a primary aluminum industry in India. Int. *J. Occup. Environ. Med.* **4**, 61-72.

Takuma, S. (1969) Electron microscopy of the mineralization of human and rat enamel, In: Araya, S., *et al.* (eds) *Hard Tissue Research,* pp. 227-249, Ishiyaku shuppan, Tokyo.

Travis, D.F. and Glimcher, M.J. (1964) The structure and organization of, and the relationship between the organic matrix and the inorganic crystals of embryonic bovine enamel. *J. Cell Biol.* **23**, 447-497.

VB Rao, A. and Vidyunmala, S. (2009) Cumulative effect of fluoride on hematological indices of mice, *Mus norvegicus albinus*. American-Eurasian *J. Toxicological Sciences* **1**, 81-83.

Voegel, J.C. and Frank, R.M. (1977) Stages in the dissolution of human enamel crystals in dental caries. *Calcif. Tissue Res.* **24**, 19-27.

Warburg, O. and Christian, W. (1942) Isolation and crystallization of enolase. *Biochem. Z.* **310**, 384-421.

Weiss, M.P., Vogel, J.C. and Frank, R.M. (1981) Enamel crystallite growth: width and thickness study related to the possible presence of octacalcium phosphate during amelogenesis. *J. Ultrastruct. Res.* **76**, 286-292.

Wilson, R.H. and Deeds, F. (1939) Experimental chronic cadmium poisoning. *Science* **90**, 498.